CIRCUIT-BASED ANALYSIS OF TAPPED-IN COUPLING BETWEEN COMBLINE RESONATORS APPLICABLE IN WIDEBAND FILTER DESIGNS

B. Mohajer-Iravani

EMWaveDev
1722 N College Ave, Fayetteville, AR 72703, USA

M. A. El Sabbagh

Syracuse University
Syracuse, NY 13244, USA

Abstract—We showed that creating coupling between resonators through transverse electromagnetic transmission line directly tapped into both resonators provides a viable solution for the design of wideband microwave components where strong coupling values are required. However, more analysis is needed to explain the coupling mechanism and its limitation. In this work, we present the developed equivalent circuit model which is comprised only of lumped elements for comprehensive analysis of the tapped-in coupling between planar or cavity combline resonators. The effects of lumped elements which are in correspondence to physical parameters on coupling value and resonant center frequency are derived. The circuit model predicts that this coupling mechanism by adjusting the design parameters of coupling section simply realizes any required strength of coupling between resonators, i.e., from weak values close to zero up to strong values close to unity. Therefore, wideband filters are easily designed and their bandwidth can be controlled based on inter-resonator tapped-in coupling. This fact is validated through measurements for two-coupled resonators with unloaded resonant frequency of 1.45 GHz. The bandwidth is extended to 90% via tapped-in method. The total dimensions of structure are $\lambda/4 \times \lambda/18 \times \lambda/72$.

1. INTRODUCTION

Although, the realization of input/output coupling through tapped-in feed lines is well known [1], only recently attention is paid to the potential of inter-resonator coupling created through tapped-in method. In [2] and [3], it was proposed to realize strong coupling values between combline resonators through a transmission line directly tapped into resonators to be coupled. The coupling transmission line operates in transverse electromagnetic (TEM) or quasi-TEM mode. This new method of coupling differs from the well-known conventional coupling through gap or iris [4].

The numerical analysis carried out in [3] showed that inter-resonator tapped-in coupling simply realizes a broad range of coupling up to high values close to unity. This achievement in coupling strength cannot be obtained by means of conventional coupling methods. In addition, the study in [3] demonstrated that the strength of the coupling is controlled by the design parameters of the coupling section. This method can easily create the strong coupling required in design of wide/ultra-wideband microwave components such as filters.

In [5], a simple circuit model comprised only of lumped elements is developed to model the inter-resonator tapped-in coupling mechanism between symmetric resonators. Here, this circuit model is used to explain the behavior of coupling phenomena and its relation to the physical parameters of coupling section. Mathematical relations are derived to express the coupling and resonant frequency in terms of the circuit-model elements. The derivatives of these expressions are used to describe the behavior of the coupling and resonant frequency in term of circuit elements. The circuit model explains the coupling mechanism and the limits of coupling strength that can be achieved. It is noted that the circuit model and the results introduced here are used in the development of circuit-based CAD tool to speed up the design of microwave combline filters. Finally, measurement results are provided to confirm the simplicity of adjusting coupling strength between combline resonators using the proposed coupling mechanism.

2. CIRCUIT MODEL AND ANALYSIS

As a simple and basic study case, we consider two identical combline resonators coupled based on tapped-in TEM transmission lines. The total structure is symmetric as shown in Figure 1(a) for the cavity combline resonators and Figure 1(b) for planar combline resonators. The corresponding equivalent circuit model is shown in Figure 1(c) where metallic and dielectric losses are neglected. The unloaded
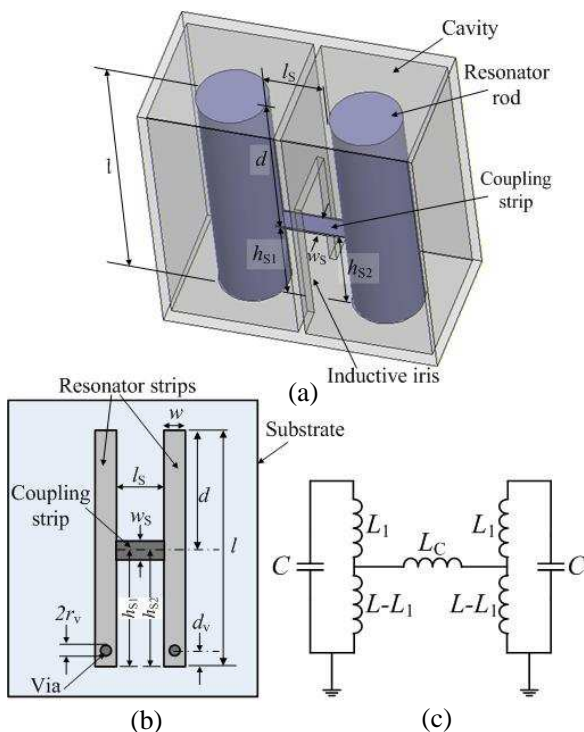
Figure 1. (a) 3-D view of two symmetric cavity combline resonators coupled through strip tapped into resonators. (b) Top view of two symmetric planar combline resonators coupled through tapped-in strip. Design parameters are shown. (c) Corresponding equivalent circuit model made only of lumped elements.

resonant frequency F_0 of each individual resonator is modeled as the parallel combination of inductance L and capacitance C where $F_0 = 1/(2\pi\sqrt{LC})$. L and C represent the equivalent inductance and capacitance of resonator, respectively. L_1 is the inductance of the partial length of a resonator between the junction of direct connection of coupling strip to the resonator and the open end of each resonator. This part of resonator has a length $d = l - h_S$ where $h_S = h_{S1} = h_{S2}$ for the symmetric configurations. l is the total length of each resonator and h_S is the part of resonator between the shorted end and coupling strip junction. The coupling transmission line is modeled as a pure inductance L_C (capacitance between coupling strip and ground is not included to simplify the modeling). It is noted that the basic relationships between the design parameters of basic transmission lines
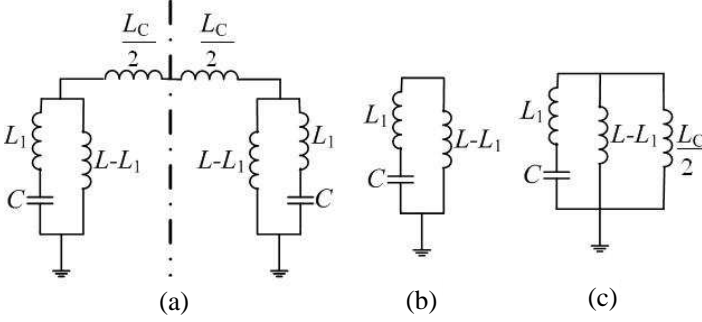
Figure 2. (a) Rearranged equivalent circuit of the model given in Figure 1(c). Symmetry line is defined in this circuit model. (b) Equivalent circuit model for even symmetry. (c) Equivalent circuit model for odd symmetry.

and lumped elements equivalently modeling them are well documented in modeling references such as [6]. In the next section, some of these functions are presented.

The elements of the circuit model shown in Figure 1(c) are rearranged to represent the circuit model shown in Figure 2(a). This model is used to compute the coupling k between two symmetric resonators and the corresponding resonant center frequency f_0. For these computations, only half of the circuit model marked with symmetry line is solved for the two cases corresponding to a circuit with even symmetry as shown in Figure 2(b) and a circuit with odd symmetry as shown in Figure 2(c). An analysis of the circuit model with even or odd symmetry is equivalent to the numerical study of the physical structure of a coupled resonators shown in Figure 1(a) or (b) with a perfect magnetic wall or a perfect electrical wall, respectively, placed at the symmetry plane. The resonant frequencies of the circuit due to even and odd symmetries are determined and denoted as magnetic resonance f_m and electric resonance f_e, respectively. It is noted that k and f_0 are related to these resonances as follows [4]:

$$k = (f_e^2 - f_m^2)/(f_e^2 + f_m^2) \tag{1}$$
$$f_0 = \sqrt{f_e f_m}. \tag{2}$$

The resonant frequency of the circuit with even symmetry is identical to the unloaded resonant frequency of single resonator, i.e., $f_m = F_0$. Thus, the magnetic resonance does not change with loading.

The resonant frequency of the circuit with odd symmetry is

$$f_e = 1/2\pi\sqrt{L_e C} \tag{3}$$

$$L_e = L_1 + \left\{ (L - L_1) \| \frac{L_C}{2} \right\} \tag{4}$$

where the symbol $\|$ means parallel combination. L_e is the equivalent electric inductance of the circuit with odd symmetry. Further, L_e is less than L. Hence, $f_e > F_0$ or $f_e > f_m$ and this indicates that the proposed inter-resonator tapped-in coupling is inductive ($k > 0$) as mentioned in [3].

f_e increases by decreasing L_e and f_e dominantly affects k and f_0. This is explained through the first-order derivative of these parameters with respect to f_e as follows:

$$\partial k / \partial f_e = \frac{4 f_e f_m^2}{(f_e^2 + f_m^2)^2} \tag{5}$$

$$\partial f_0 / \partial f_e = \frac{1}{2}\sqrt{f_m / f_e}. \tag{6}$$

The derivatives are positive. Thus, the coupling and the resonant center frequency increase with an increase of electric resonant frequency.

The inductance L_e is a function of the two variables L_1 and L_C. The first-order derivative of L_e with respect to L_1 indicates the effect of L_1 on L_e as follows:

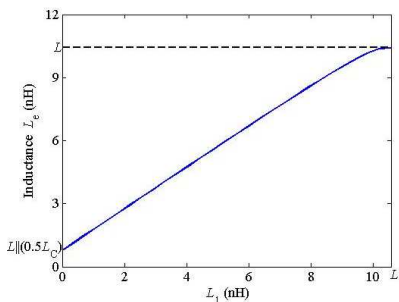$$\partial L_e / \partial L_1 = 1 - (L_C / D)^2 \tag{7}$$

Figure 3. Equivalent electric inductance L_e versus L_1 for the circuit with odd symmetry shown in Figure 2(c). The values of lumped elements are $L = 10.44\,\text{nH}$ and $L_C = 1.74\,\text{nH}$.
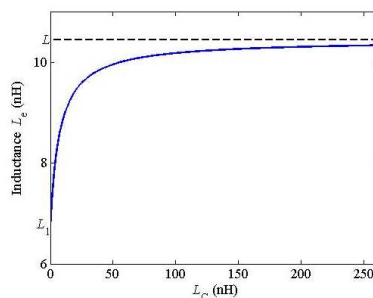
Figure 4. Equivalent electric inductance L_e versus L_C for the circuit with odd symmetry shown in Figure 2(c). The values of lumped elements are $L = 10.44\,\text{nH}$ and $L_1 = 6.73\,\text{nH}$.

where $D = 2(L - L_1) + L_C$. D is always greater than L_C and $(L_C/D) < 1$. Therefore, this derivative is always positive and its value decreases as L_1 increases. Hence, L_e continuously increases versus L_1 as the example presented in Figure 3 shows. L_e changes from $[L\|(L_C/2)]$ to L as L_1 increases from 0 to L. The first-order derivative of L_e with respect to L_C shows the behavior of L_e versus L_C. This derivative is

$$\partial L_e/\partial L_C = 2((L - L_1)/D)^2. \tag{8}$$

The slope of L_e in (8) is positive, yet, it decreases with increasing L_C (i.e., D increases). Therefore, L_e increases by increasing L_C as shown through the example presented in Figure 4. As L_C varies from 0 to ∞, L_e changes from L_1 to the asymptote value L. The values of the lumped elements in the circuit model used to plot Figures 3 and 4 are $L = 10.44\,\text{nH}$ and $C = 1.16\,\text{pF}$ which results in an unloaded resonant frequency $F_0 = 1.45\,\text{GHz}$, $L_C = 1.74\,\text{nH}$, and $L_1 = 6.73\,\text{nH}$.
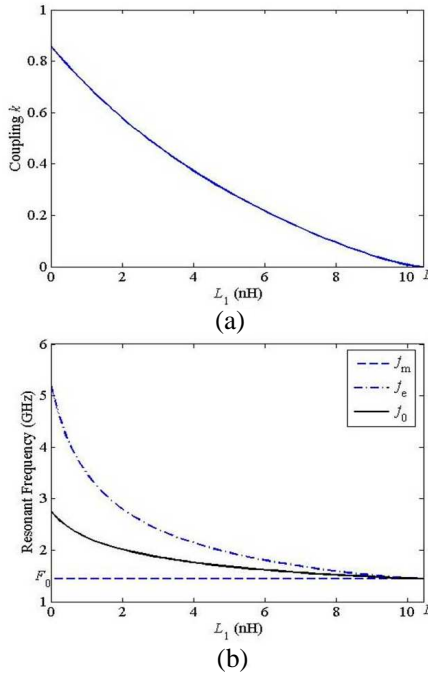

(a)

(b)

Figure 5. (a) Magnetic coupling versus L_1 and (b) magnetic, electric, and center resonant frequencies versus L_1 obtained from the circuit models shown in Figure 2. The values of lumped elements are $C = 1.16\,\text{pF}$, $L = 10.44\,\text{nH}$, and $L_C = 1.74\,\text{nH}$.

Thus, as L_1 or L_C decreases: L_e decreases based on (7) and (8); f_e increases according to (3); and both k and f_0 increase in accordance with (5) and (6). Figure 5(a) shows the coupling k versus L_1 for the circuit model under study. The coupling curve illustrates that it is possible to realize a broad range of coupling values from nearly zero up to unity based on the direct connection of resonators through the coupling transmission line. For this example, the maximum achieved coupling is equal to 0.85 and the minimum coupling theoretically goes to zero as L_1 asymptotically reaches L, which indicates uncoupled resonators. For the same circuit model, the graphs of f_m, f_e, and f_0 versus L_1 are presented in Figure 5(b). A significant change of resonant frequency versus L_1 is observed. The resonant frequency follows the same trend as coupling. The large variation of resonant frequency mostly occurs at small values of L_1 which provides strong coupling.

It is noted that if the equivalent circuit model of two coupled resonators is not symmetric, then two resonant frequencies extracted from the analysis of total circuit replace f_m and f_e in (1) and (2) to compute k and f_0. These values are similarly controlled by the design parameters of coupling section or the equivalent lumped elements in the model.

All analysis carried out shows that the appropriate selection of lumped-element values provides the required coupling between any two resonators in the filter structure. This allows for flexibility in adjusting bandwidth from narrow to wide.

3. COUPLING VERSUS PHYSICAL DESIGN PARAMETERS

In this section, we investigate the relationship between the coupling as well as the resonant center frequency and the design parameters of coupling section for coupled planar combline resonators shown in Figure 1(b). These design parameters are coupling strip length l_S, its width w_S, and the tapped-in locations along the resonators measured from shorted ends h_S. In our circuit modeling, dielectric and metallic losses are neglected. Low-loss materials which are used in high-frequency designs justify this assumption. Also, the metallization is considered to be zero thickness. The value of L_1 is defined by

$$L_1 = L_P + L_{MIP} \qquad (9)$$

L_P is the self inductance of the partial section of resonator strip with length d. L_{MIP} is the mutual inductance between this part of resonator strip and its ground image [7]. This mutual inductance accounts for the effects of ground plane on the resonator strip. The self inductance

of strip is given by [6, 8]

$$L_P = \frac{\mu_0}{2\pi} l_{eff} \left[\ln\left(\frac{l_{eff}}{w_{eff}}\right) + 1.193 + 0.2235 \frac{w_{eff}}{l_{eff}} \right] \qquad (10)$$

where in our study it is assumed that the effective strip width $w_{eff} = w$ and its effective length is $l_{eff} = d$ (in fact, the effective length is less than length d, for more discussion refer to Appendix). The substrate material is non-magnetic $\mu_r = 1$ and μ_0 is the permeability of free space. The mutual inductance is computed using Greenhouse formula [9]

$$L_{MIP} = -\frac{\mu_0}{2\pi} l_{eff} \left[\ln\left(\frac{l_{eff}}{2h} + \sqrt{1 + \left(\frac{l_{eff}}{2h}\right)^2}\right) - \sqrt{1 + \left(\frac{2h}{l_{eff}}\right)^2} + \frac{2h}{l_{eff}} \right]. \quad (11)$$

In (11), the term $2h$ which is twice the substrate height represents the distance between the actual resonator strip and its image. The actual strip and its image have opposite current flow. This explains the negative sign of mutual inductance. As the ground plane moves closer to resonator strip, the inductance L_1 decreases. Formula (9)–(11) show that the inductance L_1 decreases by pushing the coupling strip tapped-in location toward the open end of resonator. That means, if h_S increases (d and l_{eff} decrease), then L_1 decreases and based on discussion in Section 2: L_e decreases, f_e increases, and both k and f_0 increase.

The inductance L_C of coupling strip is computed using the same formula for L_1 where $w_{eff} = w_S$ and $l_{eff} = l_S + w$. L_C increases by lengthening the coupling strip l_S or decreasing its width w_S. Then, based on discussion on Section 2: L_e increases, f_e decreases, and both k and f_0 decrease.

Similar results for the cavity combline resonators shown in Figure 1(a) are also concluded. Increasing h_S by pushing the coupling strip tapped-in junctions toward the open end of rod resonators leads to decrease of L_1. Decreasing the length of coupling strip or increasing its width causes L_C to decrease. Hence, L_e decreases; f_e increases; k and f_0 increase. Any TEM-coupling transmission line with other configuration gives similar results. The above mentioned trends and conclusions agree with those reported in [3].

Following, we compare results obtained from the developed equivalent circuit model with those extracted from numerical full-wave simulation using Ansoft HFSS [10] which are reported in [3]. The results of f_e and f_m from both methods are shown in Figure 6. The design parameters of planar coupled combline resonators are $w = 2 \, \text{mm}$, $l = 28.8 \, \text{mm}$, $d_v = 0.7032 \, \text{mm}$, $r_v = 0.2032 \, \text{mm}$. The dielectric

Rogers laminate RO4003C has a thickness $h = 1.524$ mm, relative permittivity $\varepsilon_r = 3.55$ and loss tangent $\tan \delta = 0.0027$. The unloaded resonant frequency $F_0 = 1.45$ GHz. Dimensions of coupling strip are $w_s = 1$ mm, $l_s = 2.2$ mm, and $h_{s1} = h_{s2} = h_s$ which varies from 1.5 mm to 18.5 mm. Values of all lumped elements in the model are calculated using (9)–(11) and (A-1)–(A-5). The curve of f_m obtained from full-wave analysis verifies that its changes versus h_S are negligible and it is quite equal to f_m obtained from the equivalent circuit model, which is equal to F_0. The curves for f_e confirm that f_e increases versus h_S. The results from this simple equivalent circuit model do not fully agree with HFSS but they validate the concept (discussion about identifying the effective resonator length that improves the results extracted from the circuit model is presented in the Appendix). In similar way, the results produced by the model through the variation of coupling strip width w_s or length l_s validate the trend of results extracted by full-wave analysis.

In Figure 6, the HFSS results which resemble the actual scenario converge to a frequency higher than F_0 as $h_s \to 0$. The reason is explained as follows. The via connection at the end of resonator does not represent the real ground. In reality, the via extends through the dielectric substrate between the actual ground and resonator strip. Therefore, at this point, coupling between resonators through the
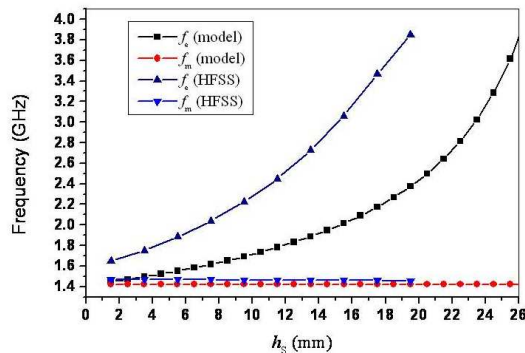

Figure 6. Magnetic and electric resonant frequencies versus h_S for the coupled planar resonators shown in Figure 1(b). These frequencies are extracted by two methods: 1) The developed equivalent circuit model and 2) the full-wave numerical simulator HFSS from [3]. The design parameters are $w = 2$ mm, $l = 28.8$ mm, $d_v = 0.7032$ mm, $r_v = 0.2032$ mm, $w_s = 1$ mm and $l_s = 2.2$ mm. The grounded substrate has thickness $h = 1.524$ mm, $\varepsilon_r = 3.55$, and $\tan \delta = 0.0027$.

tapped-in transmission line still exists. Theoretically speaking, even if this tapped-in transmission line is transferred to the other via end on actual ground plane then the coupling will not be zero as the coupling through gap between resonators becomes effective and dominant.

Although, this simple circuit model is not rigorous but its development is the first step in developing the circuit-based CAD tool which is useful to speed the initial wideband filter design. By enhancing the CAD tool, the full-wave simulations are only carried for the final optimization of the total filter structure.

4. FABRICATION AND MEASUREMENTS

In general, the order of a filter is determined based on required specifications such as bandwidth, selectivity, and return loss. In this work, our purpose is not to design a filter. Only, two-coupled resonators are used to study the behavior of tapped-in coupling mechanism. The dimensions of fabricated planar combline resonators based on Rogers laminate RO4003C, which are coupled via tapped-in coupling as shown in Figure 1(b), are: $w = 2\,\text{mm}$, $l = 30\,\text{mm}$, $l_S = 2\,\text{mm}$, $r_v = 0.2032\,\text{mm}$, $d_v = 0.7032\,\text{mm}$, and dielectric thickness is $1.524\,\text{mm}$. The dimensions of structure at resonant frequency $1.45\,\text{GHz}$ are $\lambda/4 \times \lambda/18 \times \lambda/72$. To show only the strength of inter-resonator coupling versus the design parameters of coupling section, the input/output 50-Ω feed lines are loosely coupled to the resonators, i.e, the input and output coupling are not optimized to give a good return loss. The location of tapped-in coupling strip along the resonators and its width are changed and the effect of these changes on bandwidth is measured.
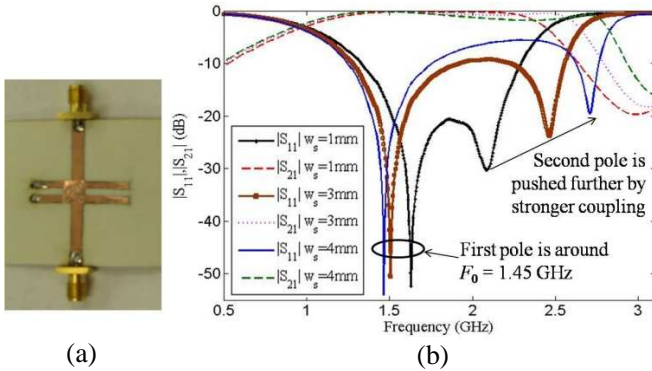

(a)   (b)

Figure 7. (a) Fabricated structure. (b) Measurements for different samples of coupled combline resonators.

Figure 7 shows a fabricated test structure and the frequency responses of three different coupling setups: $h_S = 10.5\,\text{mm}$ and $w_S = 1\,\text{mm}$, $h_S = 11.5\,\text{mm}$ and $w_S = 3\,\text{mm}$, and $h_S = 12\,\text{mm}$ and $w_S = 4\,\text{mm}$. It is observed that by increasing h_S (i.e., decreasing L_1) and increasing w_S (i.e., decreasing L_C) the first pole of each structure locates close to the resonance of each individual resonator $F_0 = 1.45\,\text{GHz}$. However, the second pole is pushed further away from the first pole as the coupling gets stronger. For the first to third setups, the second pole resonates at $2.0\,\text{GHz}$, $2.5\,\text{GHz}$, and $2.75\,\text{GHz}$, respectively. The second pole in the third setup is pushed away from the first pole by 90% through tapped-in coupling. It is noted that while the bandwidth is increasing, the return loss is getting worse. As we are investigating only inter-resonator coupling phenomena, we cannot change simultaneously the input/output coupling which affects the return loss (matching). The results show that by properly changing the physical parameters of coupling section it is possible to obtain strong coupling values needed in design of wideband filters.

5. CONCLUSIONS

In this work, the comprehensive analysis of coupling mechanism and its limitations for combline resonators coupled through tapped-in TEM transmission line is presented. The concepts and conclusions included herein are valid for both planar and cavity combline resonators. The analysis and discussions are based on developed equivalent circuit modeling the physical structure. The effects of lumped elements which are functions of design parameters of physical structure on coupling value and resonant center frequency are studied. The results confirm the possibility to achieve a wide range of coupling varying from zero to unity. A strong coupling is created by pushing the tapped-in junctions toward the open end of resonators, increasing the width, or decreasing the length of tapped-in transmission line. The strong coupling results in intensive increase of the corresponding resonant center frequency. The measurement results for two-coupled planar resonators based on tapped-in coupling method verify the concepts. Therefore, this tapped-in coupling between resonators is an asset in designs of wideband filters.

The developed circuit model is useful for early stages of design. The circuit model speeds up the realization process of finding the initial physical dimensions of resonators and coupling strip which satisfy the required coupling matrix and resonant center frequency. Following, full-wave analysis is performed for the final optimization of total filter structure.

APPENDIX A.

In the model presented in Figure 1(c), the total inductance of planar combline resonator shown in Figure 1(b) is defined by

$$L = L_R + L_v \tag{A1}$$

where L_R is the inductance of planar resonator strip on top of grounded substrate (microstrip part). L_v is the inductance of via shortening the resonator strip to ground plane. L_R is obtained using the same formula for L_1 (9)–(11) where the effective length of unloaded resonator strip l_{eff} is $l - d_v$. The effective width w_{eff} is w. Inductance L_v of via of radius r_v is computed using the following formula [11].

$$L_v = \frac{\mu_0 h}{2\pi} \left(\ln \frac{2h}{r_v} - 1 \right). \tag{A2}$$

This formula is also applicable for computing the inductance of rod in cavity based resonators.

The equivalent capacitance C of resonator is approximated as a parallel plate capacitance between the resonator strip and the ground plane. C is given by

$$C = \varepsilon_0 \varepsilon_r \frac{wl - \pi r_v^2}{h}. \tag{A3}$$

L_1 is the inductance of the partial length of resonator defined by d in Figure 1(b). As mentioned in Section 3, the effective length of this portion is less than the actual length, i.e., $l_{eff} < d$. This is due to several facts including the following reasons. The lumped element models are valid at low frequencies. There are high frequency effects in the structure that this model does not cover them. The current distribution on the microstrip resonator is not uniform. The current is more concentrated at the shorted end of resonator. The resonator has an open end which the electric field or the capacitance is stronger over there. Also, there is a step discontinuity at the junction between coupling strip and each microstrip resonator. One solution to this model deficiency is the introduction of a correction term as $l_{eff} = d - l_{cor}$. This correction term can be obtained by fitting a formula to the different sets of data computed from numerical full-wave analysis. This formula is the function of the physical parameters of microstrip resonator and the ratio of strip widths at the junction discontinuity. A very trivial example which is valid for our different numerical sets of data and it is only developed for demonstration purposes is

$$l_{cor} = \frac{\lambda_{0,eff}}{16} \sum_{n=0}^{\infty} \left(\frac{w_S}{l} \right)^{2n} \tag{A4}$$
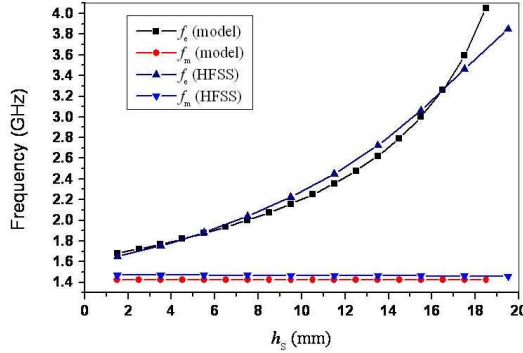
Figure A1. Magnetic and electric resonant frequencies versus h_S for the coupled planar resonators.

where $\lambda_{0,eff}$ is the effective wavelength computed at unloaded resonant frequency as

$$\lambda_{0,eff} = \frac{c}{F_0\sqrt{\varepsilon_{r,eff}}}. \tag{A5}$$

c is the speed of light in free space and $\varepsilon_{r,eff}$ is the effective relative dielectric constant of the microstrip resonator. Figure A1 shows the results of f_e and f_m from HFSS and the improved model.

REFERENCES

1. Cristal, E. G., "Tapped-line coupled transmission line with applications to interdigital and combline filters," *IEEE Trans. Microw. Theory Tech.*, Vol. 23, No. 12, 1007–1012, 1975.

2. Mohajer-Iravani, B. and M. El Sabbagh, "Ultra-wideband compact novel combline filters," *Proc. IEEE Int. Symp. Electromagn. Compat.*, 176–179, Austin, TX, 2009.

3. Mohajer-Iravani, B. and M. A. El Sabbagh, "Potential of inter-resonator tapped-in coupling in design of compact-miniaturized EMI filters," *IEEE Trans. Electromagn. Compat.*, Vol. 52, No. 1, 64–74, 2010.

4. El Sabbagh, M., K. A. Zaki, H.-W. Yao, and M. Yu, "Full-wave analysis of coupling between combline resonators and its applications to combline filters with canonical configurations," *IEEE Trans. Microw. Theory Tech.*, Vol. 49, No. 12, 2384–2393, 2001.

5. Mohajer-Iravani, B. and M. A. El Sabbagh, "Analysis of tapped-in coupling between combline resonators applicable in wideband filter designs," *IEEE Proceedings of International Conference on Wireless Information Technology and Systems*, Honolulu, Hawaii, USA, 2010.

6. Wadell, B. C., *Transmission Line Design Handbook*, Artech House, Norwood, MA, 1991.

7. Krafcsik, D. M. and D. E. Dawson, "A closed-form expression for representing the distributed nature of spiral inductor," *IEEE Microwave and Millimeter-wave Monolithic Circuits*, Vol. 86, No. 1, 87–92, 1986.

8. Bahl, I. J., *Lumped Elements for RF and Microwave Circuits*, Artech House, Norwood, MA, 2003.

9. Greenhouse, H. M., "Design of planar rectangular microelectronic inductors," *IEEE Trans. Parts, Hybrids, and Packaging*, Vol. 10, No. 2, 101–109, 1974.

10. High Frequency Structure Simulator (HFSS), Ansoft Corporation, Pittsburgh, PA.

11. Grover, F. W., *Inductance Calculations: Working Formulas and Tables*, D. Van Nostrand Company, New York, 1946.